Regional NO$_x$ emission strength for the Indian subcontinent and the impact of emissions from India and neighboring countries on regional O$_3$ chemistry

T. Kunhikrishnan,[1,2] Mark G. Lawrence,[1] Rolf von Kuhlmann,[1,3] Mark O. Wenig,[4] Willem A. H. Asman,[1] Andreas Richter,[5] and John P. Burrows[5]

[1] This study examines the regional NO$_x$ emission strength and influence of external emissions on O$_3$-related chemistry over the Indian subcontinent based on a three-dimensional chemistry transport model and space-based observations, following up on our earlier work on NO$_x$ chemistry over southern Asia. NO$_x$ mass and emissions from Global Ozone Monitoring Experiment (GOME) and Model of Atmospheric Transport and Chemistry–Max Planck Institute for Chemistry Version (MATCH-MPIC) over India are compared, and the uncertainties in the estimates are briefly discussed. This study also employs the concept of small-perturbation tendencies to compute the scaled sensitivities with modified NO$_x$ emissions for India and the neighboring continents. The sensitivities of NO$_x$, O$_3$, OH, and reservoir species of NO$_x$ over India to NO$_x$ emission from India, Southeast Asia, Africa, China, and the Middle East are discussed with respect to the photochemistry and the regional meteorology. Our study suggests that the mean regional NO$_x$ emission strength for India is close to 2.5 Tg(N)/yr with a seasonal maximum (~3 Tg(N)/yr) during April and minimum (~1.6 Tg(N)/yr) during winter. The changes in the O$_3$ concentrations with respect to NO$_x$ and nonmethane hydrocarbon emissions from India show that southern India is relatively more sensitive to local emission.

1. Introduction

[2] Industrialization, urbanization, rapid traffic growth and increasing levels of anthropogenic emissions have resulted in a substantial deterioration of air quality over Asia [*van Aardenne et al.*, 1999; *Horowitz and Jacob*, 1999; *Jaffe et al.*, 1999; *Levy et al.*, 1999; *Streets and Waldhoff*, 1999; *Yienger et al.*, 2000]. A recent study by *Akimoto* [2003] indicates that the NO$_x$ emission rate from Asia now exceeds the amounts emitted in North America and Europe and the trend is expected to continue over the next two decades. In contrast to the thinning of the O$_3$ layer in the stratosphere, the O$_3$ burden in the troposphere is generally increasing because of increasing emissions of precursors such as nitrogen oxides NO$_x$ (NO + NO$_2$) and volatile organic compounds (VOC). NO$_x$ and O$_3$ levels in urban air and amounts of nitrate in the aerosol particles over south Asia indicate that NO$_x$ levels are not negligible [*Lal et al.*, 2000; *United Nations Environment Programme* (*UNEP*), 2002].

[3] NO$_x$ indirectly influences the radiation budget of the atmosphere through O$_3$, which possibly represents 10–15% of the total anthropogenic greenhouse radiative forcing in the atmosphere [*Fishman et al.*, 1979; *Lacis et al.*, 1990, *Wild et al.*, 2001]. NO$_x$ also influences the oxidation capacity of the atmosphere through OH and nitrate. O$_3$ production in the troposphere is mainly due to the oxidation of CH$_4$, CO and hydrocarbons in the presence of NO$_x$ [*Crutzen*, 1974; *Chameides and Walker*, 1973]. A major uncertainty in tropical tropospheric chemistry is the quantification of NO$_x$ emissions from fossil fuel, bio fuel and biomass burning, soils and lightning. The photochemical transformation and losses of NO$_x$ are similarly uncertain.

[4] Our present knowledge of NO$_x$ and nonmethane hydrocarbon (NMHC) chemistry and their impact on regional ozone levels is limited because of the lack of observations of various trace gases, especially over India. In situ measurements are limited to certain locations over major cities or from field campaigns. These data are insufficient to assess the overall air quality of the country as a whole. It is reported that the emission of NO$_x$ due to fossil fuel burning could increase even more rapidly in the

---

[1]Department of Atmospheric Chemistry, Max Planck Institute for Chemistry, Mainz, Germany.
[2]Now at Atmospheric Science Directorate, NASA Langley Research Center, Hampton, Virginia, USA.
[3]Now at German Aerospace Center, Bonn, Germany.
[4]NASA Goddard Space Flight Center, Greenbelt, Maryland, USA.
[5]Department of Environmental Physics and Remote Sensing, University of Bremen, Bremen, Germany.

coming years. The uncertainty in our knowledge of the NO$_x$ chemistry and its influence on O$_3$ over India is a major problem in the way of developing effective pollution control strategies as well as a better understanding of the air quality of this region. However, a systematic approach to quantify the NO$_x$ emissions from local and remote sources is also difficult because of nonlinear chemical process in the atmosphere. As mentioned in our earlier study [*Kunhikrishnan et al.*, 2004a] (hereinafter referred to as K04a), we have proposed the use of the scaled sensitivity with model simulations to examine the impact of local NO$_x$ emissions over source and outflow regions. K04a indicates that moderate increase in NO$_x$ over India will not result in a significant change in O$_3$, taking into account the nonlinearity with the NO$_x$ lifetime and the OH feedback.

[5] Recent studies based on in situ observations over certain locations over India indicate that the rural atmosphere is significantly influenced by the urban emission, by transport and mixing [*Chand and Lal*, 2004; *Varshney and Agarwal*, 1992]. As the region is highly heterogeneous with respect to different climatic zones of arid and semiarid features and with respect to emissions from urban and rural areas, the overall atmospheric chemistry is complex. Synergetic use of a chemical transport model and satellite observations can provide a better understanding about the NO$_x$-related chemistry over this region.

[6] In continuation of our earlier work on Asian NO$_x$ (K04a), this study examines the regional characteristics of NO$_x$ induced chemistry over India using output from the global model, Model of Atmospheric Transport and Chemistry–Max Planck Institute for Chemistry Version (MATCH-MPIC), retrievals of the tropospheric NO$_2$ column, and corresponding emission estimates from the Global Ozone Monitoring Experiment (GOME) instrument on board the ERS-II satellite, which are described in the next section, including an examination of the quality of the O$_3$ simulation with respect to available MOZAIC profiles over India. In section 3, we present a review of NO$_x$ emissions over India, examine the regional NO$_x$ emission strengths based on the model, and discuss the uncertainties when using GOME NO$_2$ observations for deriving source strengths. Following that in section 4, a theoretical approach to examine the nonlinearity in the model runs with modified NO$_x$ emissions over India is discussed. On the basis of this, the influence of continental emissions on NO$_x$ chemistry over India in light of the seasonal meteorology and the variation of O$_3$ with respect to precursor emissions are briefly discussed.

2. GOME Satellite Observations and Global Three-Dimensional Chemical Transport Model

[7] This study uses the retrieval of tropospheric NO$_2$ columns [*Richter and Burrows*, 2002] (hereinafter referred to as RB02) along with the derived NO$_2$ emissions [*Wenig*, 2001] (hereinafter referred to as W01) from GOME. GOME is a scanning spectrometer on board the ERS-2 satellite, which was launched by the European Space Agency in April 1995. ERS-2 is in a Sun-synchronous orbit, approximately 800 km above Earth, crossing the equator at 1030 local time. Detailed descriptions of GOME NO$_2$ retrieval methods are given by *Burrows et al.* [1999]. For the

retrievals used in this work, the spectral window 423–451 nm, where NO$_2$ has strong absorption features, has been selected. GOME-NO$_2$ emission data used in this study are based on an improved algorithm (W01) following on the study of *Leue et al.* [2001]. GOME has shown its capability to observe many realistic features in the atmosphere; however, some of the drawbacks are its low resolution and the uncertainties in the retrieval techniques [*Kunhikrishnan*, 2004]. Generally, the uncertainty in GOME is the smallest for NO$_2$ source regions and high-albedo regions (RB02) and is typically of the order of 4×10^{14} molecules/cm^2.

[8] This study also employs data from a simulation with the three-dimensional global chemistry-meteorology model MATCH-MPIC version 3.1, at a horizontal resolution of T21, 28 vertical levels from surface to 2.7 hPa and a time step of 30 min. Details of the chemical and physical processes in the model are given by *Lawrence et al.* [1999, 2003], *von Kuhlmann et al.* [2003a, 2003b], and *Rasch et al.* [1997]. MATCH is an offline chemistry transport model with driving meteorology from the NCEP/NCAR Reanalysis data [*Kalnay et al.*, 1996]. The model uses the basic meteorological parameters such as pressure, temperature, and wind, which are used to compute the convective transport, cloud microphysics, including cloud fraction for both convective and nonconvective clouds, cloud water and precipitation. The model is able to simulate the full hydrological cycle and determines the water vapor distribution from latent heat fluxes, transport and cloud parameters. The MATCH meteorology simulates transport by advection, convection and dry turbulent diffusion. The chemical component of the model consists of sources, sinks and chemical transformations of important trace gases, which are divided according to their lifetimes into transported and nontransported species. The model consists of 56 species with 141 gas phase reactions, out of which 33 are photolysis reactions. The chemical scheme in the model deals with photochemical reactions involving major chemical species in the troposphere related to O$_3$, HO$_x$, NO$_y$, CH$_4$, CO and VOCs up to C5 (isoprene).

[9] The sources considered in MATCH-MPIC are partly from direct emissions and partly from photochemical transformations. In addition to that, stratospheric intrusions and transport from source to receptor regions also play significant roles as sources of major trace gases. Detailed information on NO$_x$ emissions used in the model is given in K04a. Carbon monoxide (CO) emission is mainly from industrial and biogenic activities and biomass burning. The oxidation of volatile organic compounds (VOC) also contributes to the total of 2260 Tg (CO)/yr in the model. Methane (CH$_4$) is fixed in the surface layer in the model allowing transport and photochemical oxidation by OH to determine its concentration in the rest of the atmosphere [*Lawrence et al.*, 1999].

[10] Various studies have been made to evaluate MATCH-MPIC with observations from satellite, aircraft data, ozonesondes and various field campaigns over different regions [*von Kuhlmann et al.*, 2003a, 2003b; *Lawrence et al.*, 1999, 2003; *Kunhikrishnan et al.*, 2004a, 2004b]. The model has been extensively compared with observations of various species such as NO$_x$, O$_3$, and CO and was found to generally reproduce the spatial and temporal variability such as land sea gradients and seasonal cycles. These include
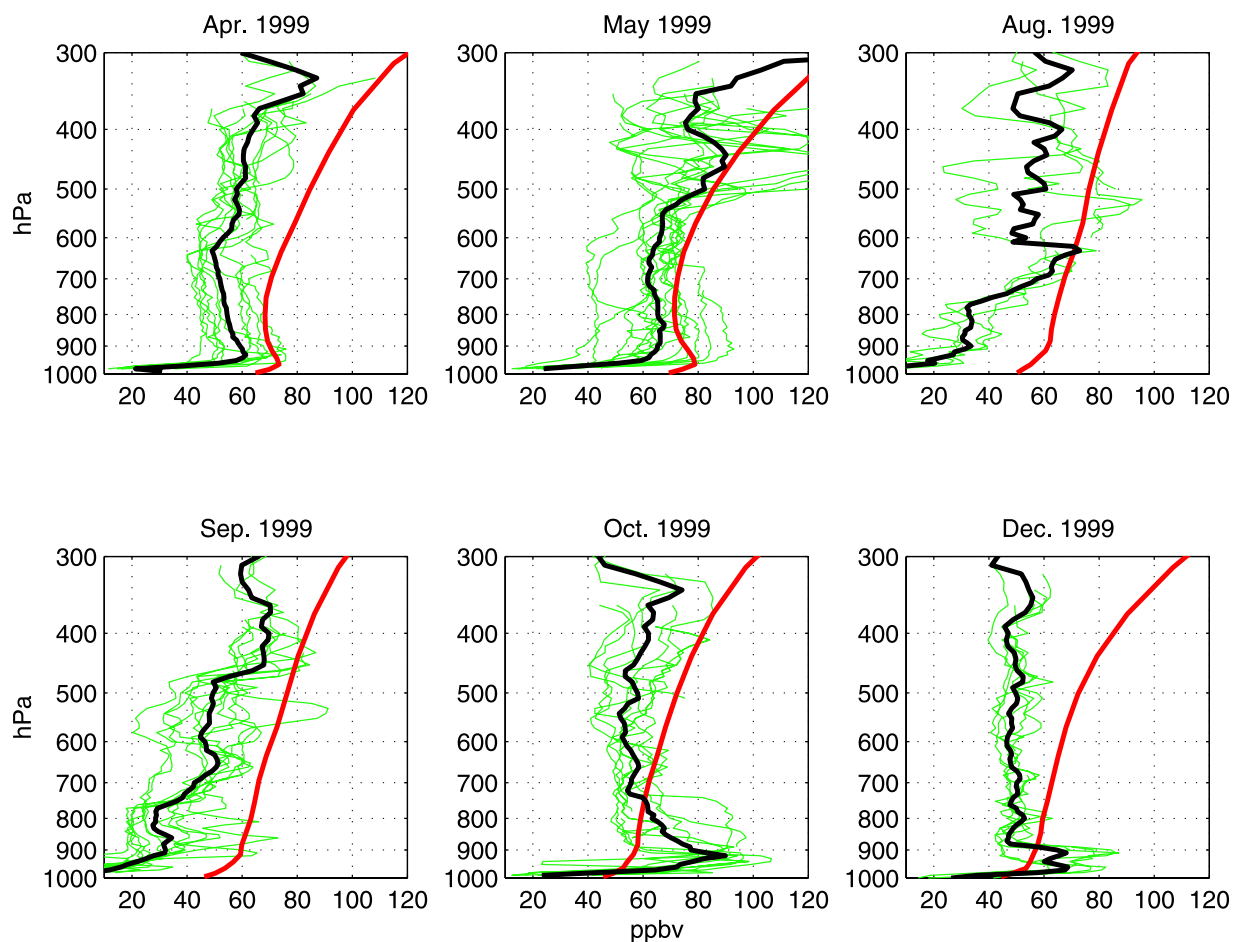
Figure 1a. O$_3$ vertical profiles (green lines) and their mean profile (black line) from MOZAIC and the monthly mean profile (red line) from MATCH-MPIC in parts per billion by volume (ppbv) for Delhi.

INDOEX data covering outflow from India [*Lawrence et al.*, 2003], a study of Asian NO$_x$, in particular over India along with the GOME NO$_2$ column (K04a) and observations from the MINOS campaign considering the transport of O$_3$ precursors from southern Asia to the Mediterranean [*Lawrence et al.*, 2003; *Lawrence*, 2004]. Over India, the magnitude of the modeled NO$_2$ column is comparable to the observations from GOME, although the model tends to underestimate the pronounced maximum during the biomass burning periods (K04a). The model is also able to reproduce the occurrence of semiregular NO$_2$ plumes in the middle troposphere (MT) over the southern Indian Ocean during the monsoon transition periods as observed by the GOME satellite [*Kunhikrishnan et al.*, 2004b].

[11] As a further step toward evaluating the model performance of O$_3$ chemistry over India, O$_3$ profiles from Measurement of Ozone by Airbus In-service Aircraft (MOZAIC) [*Law et al.*, 1998; *Marenco et al.*, 1998; *Thouret et al.*, 1998] available over this region which have been preprocessed for 1997–1999 are compared with the monthly mean 24-hour O$_3$ from MATCH-MPIC.

[12] Direct comparison between the model and MOZAIC is limited by the low model resolution and monthly averaged output as compared to the instantaneous MOZAIC profiles available over Indian airports. In this study we use vertical profiles corresponding to takeoff and landing within

a horizontal range of 200 km of 3 Indian airports which are frequented by the MOZAIC aircraft: Chennai, Delhi and Mumbai. The monthly mean concentration of O$_3$ from MATCH-MPIC (red line) is plotted (Figures 1a–1c) with available MOZAIC profiles (green lines) with their mean (black line). Generally, the O$_3$ concentration increases with respect to height, which is more predominant over Delhi as compared to Mumbai and Chennai. MOZAIC profiles typically show low mixing ratios of O$_3$ (<40 ppbv) over Mumbai and Chennai, while over Delhi it is 60–80 ppbv within 1–2 km altitude. Generally, MATCH-MPIC tends to overestimate the O$_3$ concentration as compared to MOZAIC at all levels with some exceptions during October–December for Delhi. However, MATCH-MPIC does reproduce some of the main features. In particular, the lower troposphere (LT) peak, which is frequently seen around 900 hPa, the rough overall vertical shape and the seasonality are reproduced by the model. To analyze the seasonal variations, we examined the time series at three isobaric levels in the LT close to the surface (915 hPa, Figure 2a), the transition layer (690 hPa, Figure 2b), and the midtropospheric layer (500 hPa, Figure 2c) from MOZAIC and MATCH-MPIC shown here in Figure 2 for the example of Chennai. The model simulates a seasonal cycle similar to the one observed by MOZAIC, in particular the O$_3$ maxima during the dry summer and minima during the summer
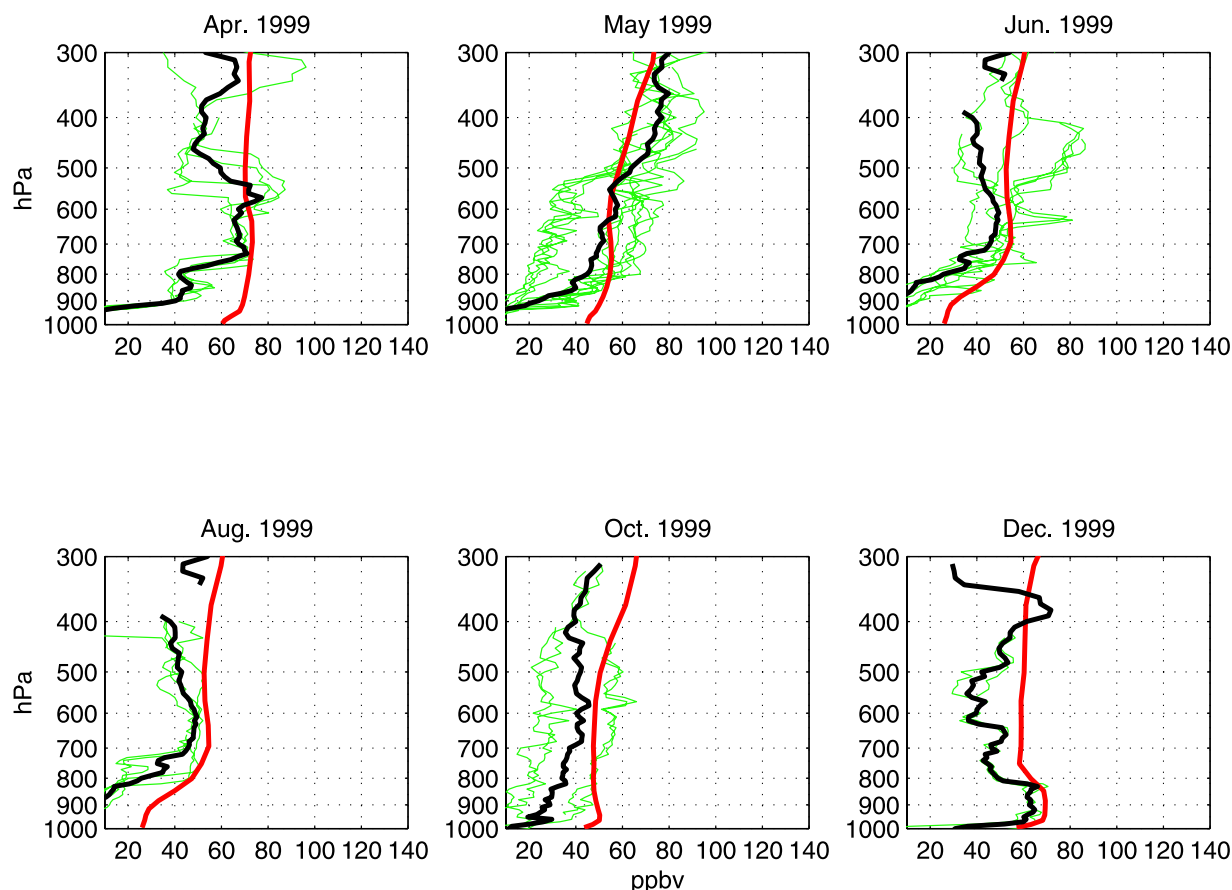
Figure 1b. O$_3$ vertical profiles (green lines) and their mean profile (black line) from MOZAIC and the monthly mean profile (red line) from MATCH-MPIC in parts per billion by volume (ppbv) for Mumbai.

monsoon months. Finally, it is interesting to note that there is not much interannual variation in the O$_3$ over these three cities on the basis of either of the data sets.

3. NO$_x$ Emission From India

[13] The chemical processes that tend to maintain the chemical composition of the atmosphere and influence climate are initially controlled or modified by the emission of trace gases. Because of the short lifetime of tropospheric NO$_x$, its regional distribution is strongly controlled by its emissions; however, in the midtroposphere (MT) to upper troposphere (UT) NO$_x$ mainly corresponds to the transport by advection and convection from remote and underlying sources. The main sources of the NO$_x$ and hydrocarbons over India are vehicular transport and biofuel burning. Power generation and industrial emissions contribute the remaining fraction. A study by *Gadi et al.* [2003] has given an estimate of 0.6–1.4 Tg for 1990 from biofuel NO$_x$ emission, which is mainly from the domestic sector of rural India that provides 70% of the total energy requirements. The increasing population and urbanization result in a 4 to 6% annual growth rate of energy consumption in India, which enhances the emissions of NO$_x$ and other trace gases [*UNEP*, 2002]. Long-term air quality data over the residential and industrial locations of different Indian cities indicate that NO$_2$ levels are increasing steadily over major cities, and some of them already exceed the permissible limits, as high

as 100 to 240 μg/m^3. Different studies based on sector analysis and measurement campaigns show that NO$_x$ emissions over India are expected to increase in the forthcoming years, even though these estimates have large uncertainties for different sectors [*Carmichael et al.*, 1998; *Garg et al.*, 2001; *Mitra and Sharma*, 2002; *Sharma et al.*, 2002; *Streets et al.*, 2003].

[14] It is clear that more efforts are needed to understand the spatial and temporal evolution of regional NO$_x$ emissions over India with respect to the increasing demand of energy consumptions, rapid urbanization and efforts to stabilize the increasing level of greenhouse gas concentrations as well as improve the air quality of this region. Data from chemistry transport models and satellites provide valuable information to improve estimates of NO$_x$ emissions as well as to identify the source regions and to study the regional O$_3$ chemistry in light of seasonal meteorology.

3.1. Regional NO$_x$ Emission Strength From MATCH-MPIC

[15] The industrial source of NO$_x$ used in MATCH-MPIC is based on the Emission Database for Global Atmospheric Research (EDGAR), version 2.0, 1° × 1° emissions inventory [*Olivier et al.*, 1999]. In the EDGAR database, the Indian emissions consist of about 64% from fossil fuel combustion and 30% from biofuel combustion, and the total NO$_x$ emission for 1995 is estimated as 1.63 Tg(N). In addition to this, the model takes into account the emission
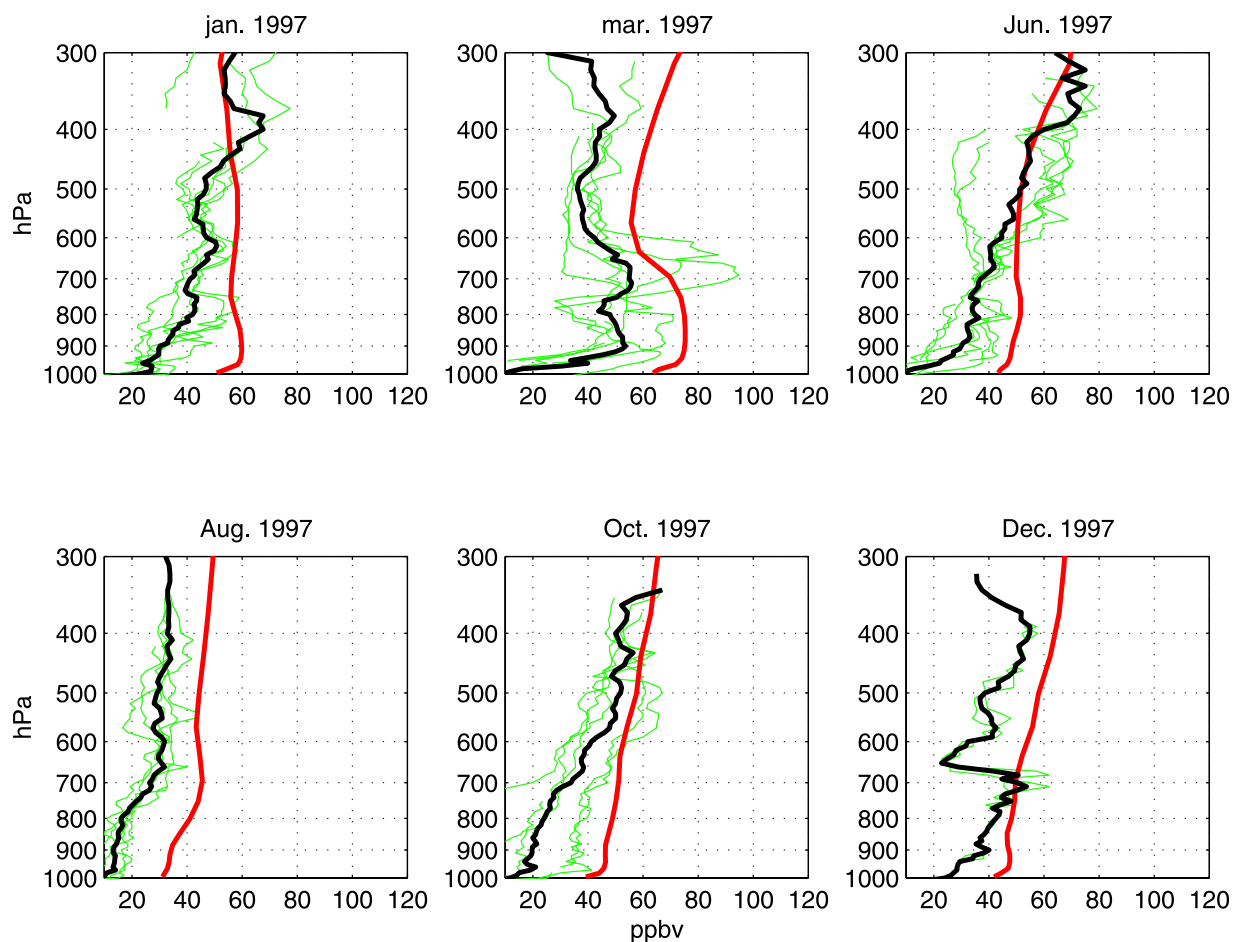
Figure 1c. O$_3$ vertical profiles (green lines) and their mean profile (black line) from MOZAIC and the monthly mean profile (red line) from MATCH-MPIC in parts per billion by volume (ppbv) for Chennai.

from soils, lightning, aircraft, biomass burning and transport from the stratosphere, which are discussed in K04a. The NMHC emissions from India consist of about 16.4% from fossil fuel combustion and 69.6% from biofuel combustion with a total national emission of 8.1 Tg(C) for 1995. NMHCs are emitted on a speciated basis, based on EDGAR data for anthropogenic emissions. The industrial and anthropogenic NO$_x$ and NMHC emissions from different sectors especially over India used in the model based on EDGAR emission data are shown in Figure 3.

[16] MATCH-MPIC shows an enhancement of NO$_x$ emissions over north to northeast India, with maximum emissions during the dry summer period of India (April) and the least during winter months (October–December). Studies based on ATSR and AVHRR satellite observations show that NE India, especially Orissa and West Bengal, are the regions of most intense biomass burning in India during March–April [*Duncan et al.*, 2003]. The Indian NO$_x$ emissions used in MATCH-MPIC for India are discussed in comparison to GOME in section 3.4. The mean NO$_x$ emission for India used in the model is 2.28 Tg(N) for 1997–1998 with a monthly standard deviation of 0.44 Tg(N).

[17] In the following section, we examine the integrated mass of NO$_2$ over India and the seasonal variation of the

NO$_x$ lifetime with uncertainties from the model, which are the main parameters that are used for computing the emission strength based on satellite data.

3.2. Vertical Distribution of Integrated NO$_2$ Mass Over India

[18] Knowing the NO$_2$ mass abundance in the troposphere enables us to estimate the emission strength for a region. For species like NO$_2$, which are present in both the troposphere and the stratosphere, the retrieval of the tropospheric contribution by satellite remote sensing is difficult. As such estimates are not easily available from satellite measurements here we examine the fraction of NO$_2$ mass in different levels of the troposphere over India by using the model; The integrated mass of the NO$_2$ column for five isobaric levels, the boundary layer (BL; surface to 850 hPa), MT (850–500 hPa), UT (500–150 hPa), tropospheric column (surface to 150 hPa) and the stratospheric column (150–2.7 hPa) are computed for the model grids corresponding to the Indian domain. The ratios of mass computed for different levels are summarized in Table 1. This shows that, in winter, ∼67% and in summer, ∼39% of the NO$_2$ mass in the tropospheric column is in the BL close to the source regions. This is mainly due to subsidence and lack of convective transport during winter and strong convective transport and photochemical activity during
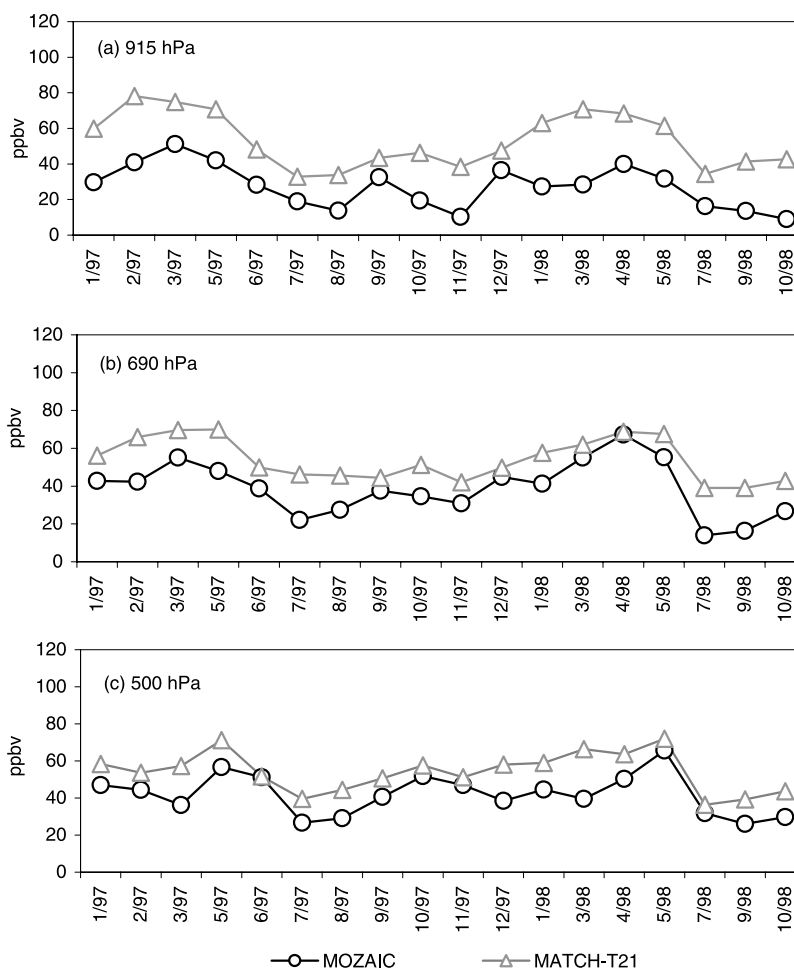
Figure 2. Seasonal variation of monthly mean O$_3$ concentration (ppbv) of available profiles from MOZAIC and MATCH-MPIC over Chennai for (a) 915 hPa, (b) 690 hPa, and (c) 500 hPa.

summer. ~30% of the NO$_2$ mass in the tropospheric column is in each of the MT and UT during summer, mainly because of convective transport and the contribution from lightning. The tropospheric mass of the NO$_2$ is less than 40% of the stratospheric NO$_2$ mass over India. As mentioned in K04a, this introduces an uncertainty with the satellite retrieval of the NO$_2$ column over this region.

3.3. Uncertainties in the Estimation of Tropospheric Lifetime

[19] The primary loss processes of NO$_x$ are the reaction with OH and the hydrolysis of N$_2$O$_5$ during nighttime. These lead to conversion to HNO$_3$, which is then lost to dry and wet deposition as described in detail by *Dentener and Crutzen* [1993] and *Crutzen and Lawrence* [2000]. This implies that the photochemical lifetime depends on OH and O$_3$, which induces spatial and temporal variations of the NO$_x$ lifetime as described in K04a. Large seasonal variations of OH associated with photochemistry and moisture transport through the monsoon circulation can be generally seen over India. In the troposphere, the source of NO$_x$ is primarily as NO. There is a rapid cycling between NO and NO$_2$ involving ozone. From the model, it is found that the NO$_2$/NO$_x$ fraction is about 0.7–0.9 in the LT and 0.3–0.5 in the UT over India (Figure 4) and this is partially the reason

for the longer lifetime of NO$_x$ in the UT (the lower OH concentration also contributes).

[20] The NO$_x$ lifetime varies spatially and NO$_x$ is recycled through PAN and HNO$_3$. The effective lifetime of NO$_x$ (NO + NO$_2$) is the average time a nitrogen atom spends as a NO$_x$ molecule between when it is emitted and when it is removed from the atmosphere (via deposition of nitrogen to the ground). This effective lifetime is different from the lifetime that is calculated on the basis of the first-order loss reactions and is difficult to quantify because it would require tracking the N through exchanges with NO$_2$, N$_2$O$_5$, HNO$_3$, PAN and other forms of NO$_y$. The most convenient way to estimate the effective lifetime is the mass-emission method (introduced in K04a), by computing the ratio of the total mass abundance of NO$_x$ over the region (taking only the 16 model columns over India) to the mean integrated emission of NO$_x$ on a monthly average basis. The assumption is that total loss rate is equal to the emission under steady state conditions. This would be the correct lifetime if there were no flux of reactive nitrogen into or out of the region. Since there is a nonzero flux, we estimate upper and lower uncertainty bars as follows. The upper limit of the lifetime is computed by taking a broader rectangular region to roughly account for the outflow of NO$_x$ from India. The lower range of the lifetime takes into account only the
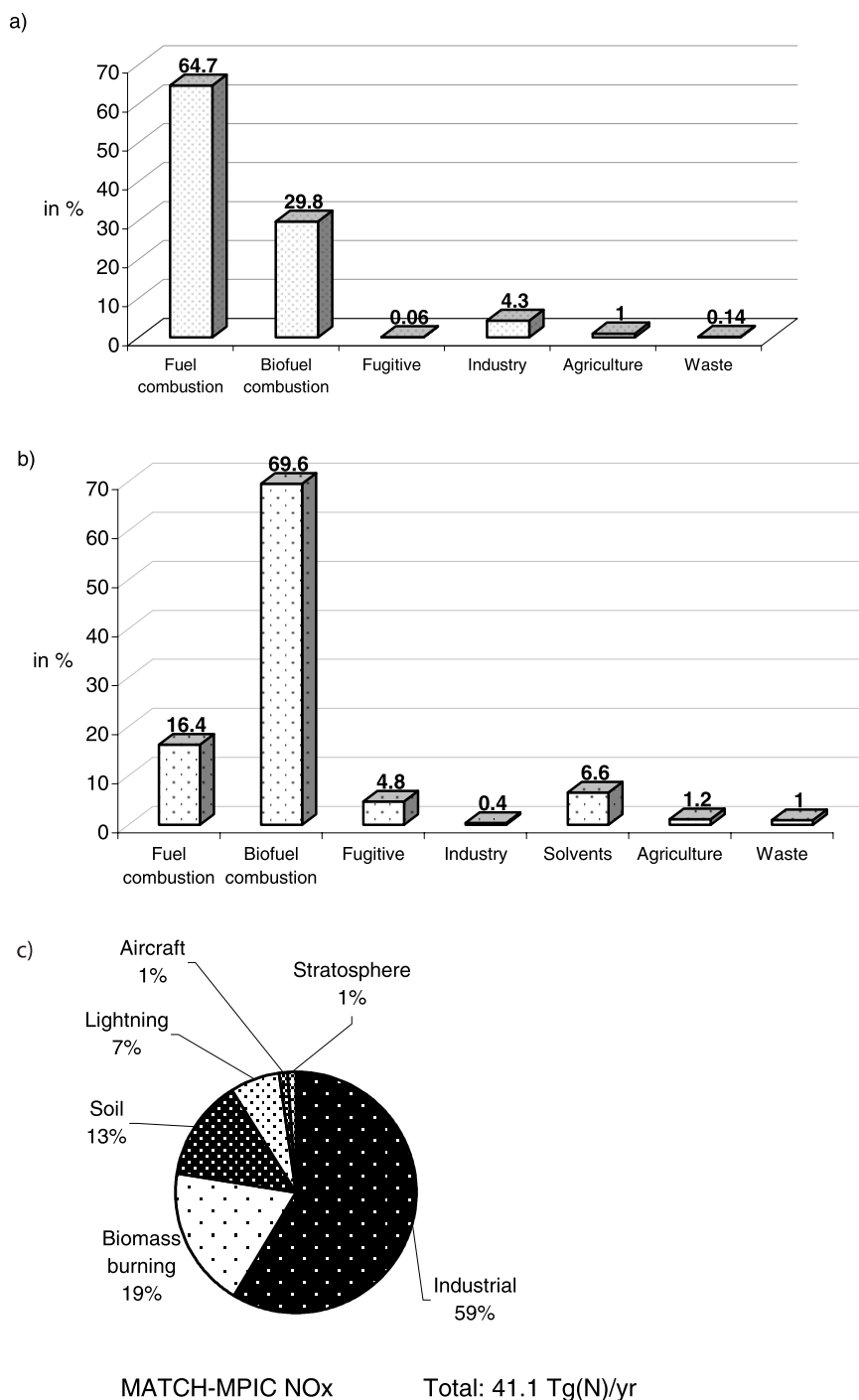
Figure 3. (a) NO$_x$ and (b) NMHC emissions over India based on EDGAR emissions inventory version 2.0. (c) Sources of NO$_x$ emissions used in MATCH-MPIC.

approximate fraction of NO$_x$, which originates from the local NO$_x$ source over India. The range of the lifetime (12–20 hours) computed in this manner is shown in Figure 5; with an estimated average uncertainty (δt) of approximately ±5 hours from mean value. The minimum values are during February–April, when the sunshine is high over India and the highest values are during October–November.

[21] Several approaches for estimating the NO$_x$ lifetime have been discussed in K04a. Here, the lifetimes of tropospheric NO$_x$ and its components computed for India

from the mass-emission method and budget analysis based on MATCH-MPIC and from the chemical decay method over the outflow region from India using GOME are summarized in Table 2. The mean lifetime of tropospheric NO$_x$ over India computed from various approaches agrees well between all the methods. However, it varies with respect to seasons on the basis of the photochemistry involving OH, solar radiation, bright sunshine hours and transport.

Table 1. Ratio of Integrated Mass of NO$_2$ Column Over the Indian Subcontinent From MATCH-MPIC

Ratio of Integrated Mass of NO$_2$[a]	January	July
BL/TC (PS to 850/PS to 150 hPa)	66.5% (1.33 × 10^9/2.0 × 10^9)	39.3% (8.2 × 10^8/2.09 × 10^9)
MT/TC (850−500/PS to 150 hPa)	23.6% (4.71 × 10^8/2.0 × 10^9)	31.1% (6.48 × 10^8/2.09 × 10^9)
UT/TC (500−150/PS to 150 hPa)	9.9% (1.97 × 10^8/2.0 × 10^9)	29.6% (6.18 × 10^8/2.09 × 10^9)
TC/SC (PS to 150/150−2.7 hPa)	40.8% (2.0 × 10^9/4.9 × 10^9)	32.5% (2.09 × 10^9/6.41 × 10^9)

[a]BL, boundary layer; MT, middle troposphere; UT, upper troposphere; TC, tropospheric column; SC, stratospheric column; PS, surface level.

3.4. Regional NO$_x$ Emission Strength From GOME

[22] Developing bottom-up emissions inventories is difficult. This is mainly due to the rapidly changing anthropogenic emissions, heterogeneity and uncertainty in detailed statistics, the lack of temporal and spatial continuity as well as the uncertainty in the natural emissions from lightning and soils. A quantitative approach to estimating the regional emission strength from space has been developed in recent years. Estimation of regional NO$_x$ emission from the GOME NO$_2$ column is described in detail by *Leue et al.* [2001], on the basis of certain assumptions. There have been several encouraging studies in this direction to quantify the NO$_x$ emission from lightning and ships based on GOME satellite observations [*Burrows et al.*, 2004; *Richter et al.*, 2004; *Martin et al.*, 2002; *Beirle et al.*, 2004].

[23] Here we first estimate the NO$_2$ emission for India based on the NO$_2$ retrieval from GOME developed in RB02. Tropospheric NO$_2$ mass from GOME over India is computed from its number density by taking an areal average. From that, NO$_2$ emission is computed for steady state conditions by taking the temporal variation of lifetime estimated from MATCH-MPIC on the basis of the mass-emission method. However, we cannot rule out biases in the new estimates, because the biases in the model emissions inherently influence the lifetime computed from the model. We found that the mean NO$_2$ source computed in this way from GOME is 0.7 Tg(N)/yr for a broader rectangular region and relatively less (0.53 Tg(N)/yr) for the Indian grids with a maximum source in the range ∼0.9−1.2 Tg(N)/yr during February−June (winter-spring). The accuracy of this value is further limited by the uncertainty (up to 50%) in the GOME retrieval especially due to clouds and aerosols during summer monsoon months.

[24] Second, we also use an estimate of NO$_x$ emission based on the GOME NO$_2$ retrieval of W01. This estimate is an improved one from GOME following on the work of *Leue et al.* [2001] with an average uncertainty of about 30−50%. In this method, the vertical column density of NO$_x$ is obtained by multiplying the retrieved NO$_2$ column by a correction factor, which also takes into account the fraction of NO$_2$ to the total NO$_x$. The conversion from NO$_2$ to NO$_x$ emissions is dependent on the photolysis frequencies, which are dependent on the solar zenith angle (SZA). If the SZA increases, the conversion factor decrease, therefore conversion factors are higher in winter than in summer. A basic assumption for computing this fraction is that NO$_2$ as measured by GOME is in photochemical stationary state with NO. The mean NO$_x$ emission from GOME for India, if we were instead to simply assume a constant lifetime of 24 hours, would be estimated at 1.63 ± 0.24 Tg(N) for 1996−2001 with a maximum of 1.75 Tg(N) for 1997. Since this estimate is based on a constant lifetime of 24 hours, it is difficult to compare directly, therefore we also compute the emission strength for India with the regionally appropriate lifetime estimated from MATCH-MPIC. The mean annual NO$_x$ emission computed for 1997−1998 from GOME is 2.35 ± 0.5 Tg(N)/yr (Figure 6) with a maximum of 3.35 Tg(N)/yr in March−April (dry summer) and a minimum of 1.65 Tg(N)/yr in November−December (winter). The NO$_x$ emission estimated from GOME is close to the mean emission (2.28 ± 0.44 Tg(N)/yr) used in MATCH-MPIC for India with a maximum of 3.03 Tg(N)/yr for the same period.

[25] As the lifetime estimate from MATCH is not free from biases due to the uncertainties as mentioned above, we
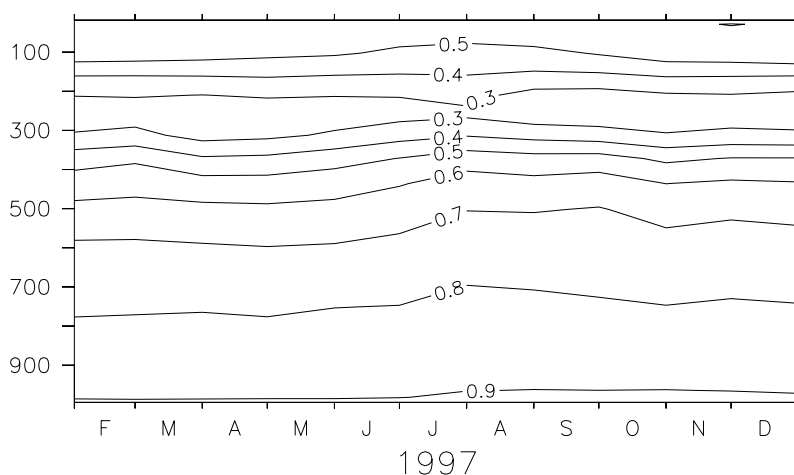
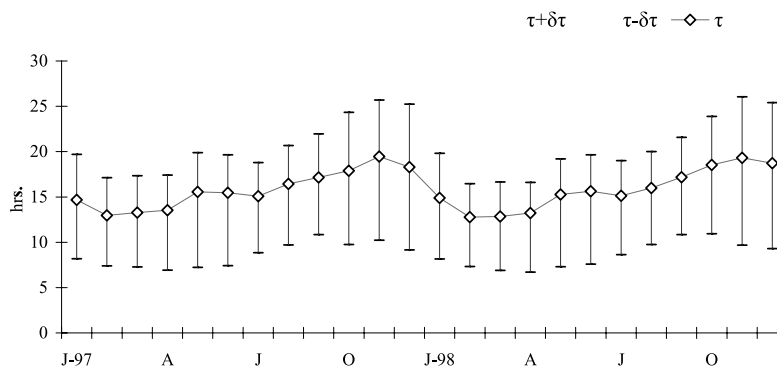**Figure 4.** NO$_2$/NO$_x$ for India from MATCH-MPIC.

Figure 5. Estimate of the tropospheric NO$_x$ lifetime over India using the mass-emission method: Uncertainties due to possible imbalances in inflow and outflow of NO$_x$ are given with error bars, the upper limit using a larger, rectangular domain including outflow region and the lower limit based on only the approximate fraction of NO$_x$ that stems from local emissions.

examine the column mass of NO$_x$ from GOME emission data (W01) and MATCH-MPIC (Figure 7). The mean NO$_x$ mass computed for India from GOME and MATCH-MPIC for 1996–2001 is $4.6 \pm 0.37 \times 10^6$ kg (N) and $4.47 \pm 0.64 \times 10^6$ kg (N) respectively, in good overall agreement. On the other hand the mass of NO$_2$ for India computed from the RB02 method is around 1.5 to 2.5×10^6 kg (N).

[26] Regional NO$_x$ emissions estimated from different methods are summarized in Table 3. The average MATCH-MPIC NO$_x$ emission for India during 1997–1998 is 2.28 Tg(N)/yr and has a maximum of 3.0 Tg(N)/yr during April, the dry summer period in India. The value is very close to the one from GOME for 1997–1998 (2.35 Tg(N)/yr with a maxima of 2.99 Tg(N)/yr). *van Aardenne et al.* [1999] have reported a value of 1.5 Tg(N) for the year 1990 based only on the anthropogenic source of NO$_x$. *Garg et al.* [2001] have estimated a higher value of 3.5 Tg(N) for 1995 from sector analysis over India. The average emission computed by *Leue et al.* [2001] from GOME using the assumption of a constant production rate and a constant lifetime (~27 hours) over India and the surrounding region is 2.96 Tg(N) for 1997. While it is clear that more effort is needed to obtain accurate estimates of the Indian NO$_x$ source, it is at least promising that several different studies and techniques now all indicate it is around 2–3 Tg(N)/yr.

3.5. Regional NO$_x$ Emission Strength From Space: Possible Uncertainties

[27] Estimation of the regional N O$_x$ emission from space is limited by the uncertainties due to many factors such as varying lifetime, external influences on the regional chemistry such as transport, and errors in the retrieval methods with varying clouds, albedo and aerosols. The model

sensitivity simulations for India discussed in K04a and section 4 indicate the influence of a nonnegligible contribution of external NO$_x$ sources, which introduces an uncertainty into the estimation of the regional NO$_x$ source strength using GOME as employed by *Leue et al.* [2001]. In addition to that, the lifetime of NO$_x$ varies with respect to space and time, having an uncertainty of ~5 hours over India, which implies that we cannot use a constant lifetime to estimate the emissions as long as the variation exceeds the uncertainty. The estimate of NO$_x$ lifetime from GOME is also restricted to only certain outflow regions.

[28] There are attempts to improve the emission estimate from GOME by taking different steps. *Martin et al.* [2003] proposed a new method to estimate the emission by taking top-down information derived from the GOME NO$_2$ column to reduce the uncertainties in NO$_x$, while trying to integrate the information from bottom-up inventories. However, this method does not include varying regional lifetimes and the uncertainty due to export/import as discussed above. Combining these various advances may eventually lead to an improved NO$_x$ emission inventory based on observations from space.

4. Impacts of NO$_x$ Emissions on Regional Tropospheric Chemistry

[29] Following up on the previous section, in which we focused on the magnitude of regional NO$_x$ emissions, in this section we examine their impact on the tropospheric chemistry of the region. We first describe the methodology for the sensitivity studies, then several aspects of the impacts of the emissions.

Table 2. Lifetime of Tropospheric NO$_x$ Over India From Different Methods Based on *Kunhikrishnan et al.* [2004a]

| Method	Lifetime of NO$_x$	Basic Assumptions	Data Source/Remarks
Mass-emission method	12–22 hours	steady state conditions; loss rate equals total emission	MATCH-MPIC
Exponential decay	ι(NO$_2$): 18.2 hours	$C(x) = C(0) \exp(-t/\iota)$; wind is a function of time; C, concentration	GOME; source region: west coast of India
Sink of NO$_x$ against HNO$_3$ formation by OH	11–34 hours	loss of NO$_2$ equals loss of NO$_x$	MATCH-MPIC
Loss rate from budget analysis	16–23 hours	total loss equals loss due to photochemistry and dry deposition	MATCH-MPIC
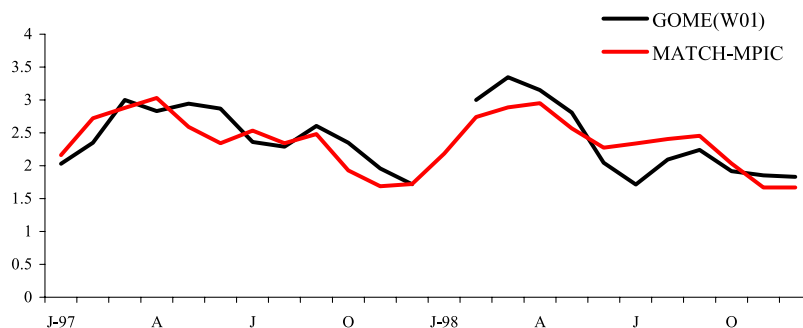
Figure 6. NO$_x$ emission [Tg(N)/yr] computed for Indian subcontinent from GOME emission estimate based on W01 (black line) and MATCH-MPIC (red line) by taking temporally varying lifetime estimates obtained from MATCH- MPIC.

4.1. Small-Perturbation Tendency: Sensitivity Studies Based on MATCH-MPIC Simulations With Indian Emissions

[30] In a previous study (K04a) we have examined the impact of NO$_x$ source perturbation for the outflow regions from India and neighboring continents to the Indian Ocean. In the present study we apply this directly for the source regions to examine their impact on India. We employ here the theory of small-perturbation tendency (SPT as proposed by *Kunhikrishnan and Lawrence* [2004]) to perform sensitivity studies to assess the impact of neighboring continental emissions on NO$_x$-related chemistry over India. The theoretical approach to the problem is described in detail with respect to perturbations in Indian NO$_x$ emissions in Appendix A. For this method, model sensitivity studies are done by taking a 10% increase of NO$_x$ emissions in a chosen region, which limits the chemical nonlinearity primarily to the first-order feedback via OH. This is then compared to the model base run results to estimate the scaled sensitivity of Indian NO$_x$ from local sources and external sources of neighboring countries. NO$_x$ responds nonlinearly to changes in emissions, since O$_3$ and OH, which depend on NO$_x$, influence its lifetime. The departure from the SPT in the LT and UT after 3 months model spin-up for December 1996 is given in Table 4. This study indicates that the relative percentage difference from the SPT for entirely masking Indian NO$_x$ (100% reduction) for the LT (surface to 500 hPa) is about 22.7% and for the UT (500−150 hPa) is 29%. Thus

there will be a deviation of ∼20−30% with a test run of 100% reduction in NO$_x$ source strength over India versus the SPT scaled sensitivity. The degree of departure is more prominent when the source strength is reduced by a factor of 50% or more, than when it is increased by the same amount especially for changes of ≥50%. This is due to the transition from a typically continental high-NO$_x$ regime to a low-NO$_x$ regime for large negative perturbations. The departure from the SPT for NO$_x$ over India becomes significant only after an increase/decrease of its source strength by a factor of 20% or more. It is clear that smaller perturbations of less than 20% in the source strength will not result in a considerable deviation from the SPT. As employed in K04a, these results show that the 10% perturbation runs can be used to directly examine the current sensitivity of NO$_x$ over India to emissions from local sources as well as to external emissions.

4.2. Sensitivity of NO$_x$ and O$_3$, OH, and PAN Over India to Continental NO$_x$ Emissions From India, Southeast Asia, the Middle East, Africa, and China

[31] In this section, we consider the impact of NO$_x$ emissions from India (60°−95°E, 7°−35°N) and the surrounding continental regions, Southeast Asia (95°−140°E, 10°S to 20°N), Africa (0°−40°E, 35°S to 35°N), China (95°−120°E, 20°−45°N), and the Middle East (35°−70°E, 10°−45°N) on NO$_x$-related chemistry over India. The surface NO$_x$ emissions during the months representing four
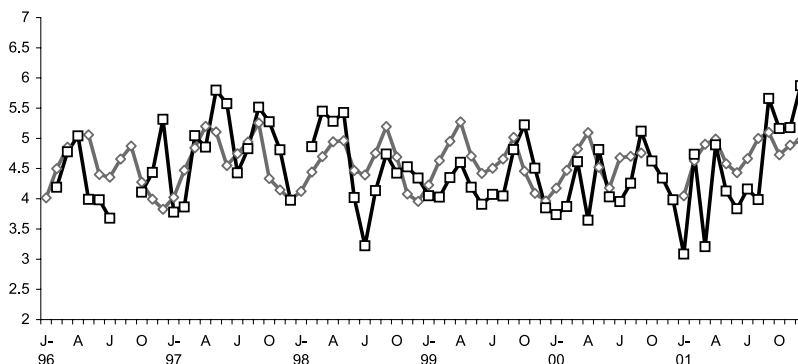

Figure 7. NO$_x$ mass in 10^6 Kg(N) for Indian region from GOME obtained from emission estimate based on W01 (black line) and MATCH-MPIC (gray line) for India, during the years 1996−2001.

Table 3. Regional NO_x Emission Strength Over India/Extended Indian Domain From Various Sources/Methods

Source	Year	NO_x Emission, Tg(N)/yr	Remarks/References
MATCH	1997–1998	2.28	lifetime, 15–20 hours
GOME-MATCH	1997–1998	2.35	lifetime, MATCH; data, GOME emission; *Wenig* [2001]
GOME	1997–1998	1.70	lifetime, 24 hours; *Wenig* [2001]
GOME	1997	2.96	lifetime, 27 hours; extended Indian region; *Leue et al.* [2001]
RAIN-ASIA	1990	1.50	based on anthropogenic source; *van Aardenne et al.* [1999]
Energy Statistics India	1995	3.55	based on sector analysis, India; *Garg et al.* [2001]

major seasons, used in MATCH-MPIC for these regions are given in Table 5. NO_x emissions are greatest for Africa (partly because of the larger area), and for China, and are lowest for the Middle East. However, annual emission per unit area from India is relatively higher compared to Africa and less than that over China. According to the EDGAR emissions statistics, Africa contributes the majority of NO_x emissions from biomass burning (∼6 Tg(N)/yr) followed by Southeast Asia (∼1 Tg(N)/yr) for 1995. NO_x from fossil and bio fuel emissions together constitute 13.7, 4.7, 4.6 and 4 Tg(N)/yr for China, Africa, the Middle East and Southeast Asia. The scaled sensitivities of NO_x, O_3, OH and PAN over India to the emissions from India, Southeast Asia, Africa, China and Middle East are computed for 1997 on the basis of runs with MATCH-MPIC in which the emissions from each region are increased individually by 10%. The results are depicted in Figure 8.

Table 4. Relative Deviations From Linearity for Different Isobaric Levels Over India From MATCH-MPIC With Respect to Changes in NO_x Abundances $[(x_1/x) - 1]$ Versus Changes in Local Source Strengths $[(f - 1)]$ for December 1996 (After a Three-Month Spin-up)

$f - 1$	$(x_1/x) - 1$	Linear Fit	Deviation	Relative Deviation, %
Surface to 850 hPa				
1	0.701	0.760	0.059	7.8
0.5	0.360	0.380	0.020	5.4
0.2	0.148	0.152	0.004	2.7
0.1	0.075	0.076	0.001	1.6
−0.1	−0.077	−0.076	0.001	−1.1
−0.2	−0.156	−0.152	0.004	−2.9
−0.5	−0.418	−0.380	0.038	−10.0
−1	−0.944	−0.760	0.184	−24.1
Surface to 500 hPa				
1	0.622	0.663	0.041	6.2
0.5	0.316	0.331	0.015	4.5
0.2	0.129	0.133	0.003	2.4
0.1	0.065	0.066	0.001	1.5
−0.1	−0.067	−0.066	0.001	−0.9
−0.2	−0.136	−0.133	0.003	−2.5
−0.5	−0.361	−0.331	0.030	−9.1
−1	−0.813	−0.663	0.151	−22.7
500–150 hPa				
1	0.080	0.088	0.008	8.9
0.5	0.042	0.044	0.002	5.3
0.2	0.017	0.018	0.001	2.2
0.1	0.009	0.009	0.001	1.1
−0.1	−0.009	−0.009	0.000	−0.8
−0.2	−0.018	−0.018	0.001	−2.4
−0.5	−0.047	−0.044	0.003	−6.8
−1	−0.113	−0.088	0.026	−29.0

[32] Tropospheric NO_x over India shows a high degree of seasonality and is mainly sensitive to emissions from local sources and neighboring continents carried to India by monsoon circulations. The largest response is to local NO_x emissions, 70–90% close to the surface for all the seasons and also in the MT to UT (∼50–70%) during the summer monsoon due to convective transport from the surface, while during winter, the sensitivity in the MT to UT to the local sources during winter is almost negligible. This implies that external emissions contribute a substantial amount of NO_x over India. Fifteen to twenty percent of NO_x in the MT to UT over India is sensitive to African NO_x during winter carried by the subtropical westerly jet (SWJ), which is more significant (10–30%) during the final phase of the 1997 El Niño when the upper air circulation was much stronger than normal years, accompanied by with the intense biomass burning over southeast Asia. The influences of emissions from Southeast Asia and China on Indian NO_x show a large seasonality with a peak during the summer monsoon of ∼25% sensitivity for NO_x in the UT due to the strong tropical easterly jet (TEJ) dominant over southern peninsular India. We also noted a sensitivity of ∼10–15% of Indian NO_x to the emissions from the Middle East carried by westerly winds in the LT during the summer monsoon.

[33] O_3 over India can also be examined with respect to NO_x emissions from the continents and NMHC emissions from India. The major contribution of continental NO_x (all together) to O_3 over India is during the summer monsoon (August–October) and is generally least responsive during the premonsoon period. The O_3 sensitivity to continental NO_x emissions takes the same pattern as NO_x (Figure 8). Twenty to twenty-five percent of BL O_3 over India is sensitive to local NO_x emissions almost irrespective of the season. The response of O_3 (∼20–30%) to local NO_x emissions can also be seen in the MT during the summer monsoon. NO_x emissions from the Middle East, Southeast Asia and China contribute ∼10% sensitivity each to O_3 over India in the LT to MT and UT during the monsoon period.

[34] The major impact of changes in NO_x emissions from India, China and South Asia together determine the overall

Table 5. Mean Surface NO_x Emission in Tg(N) Used in MATCH-MPIC for India and Neighboring Countries for the Year 1997

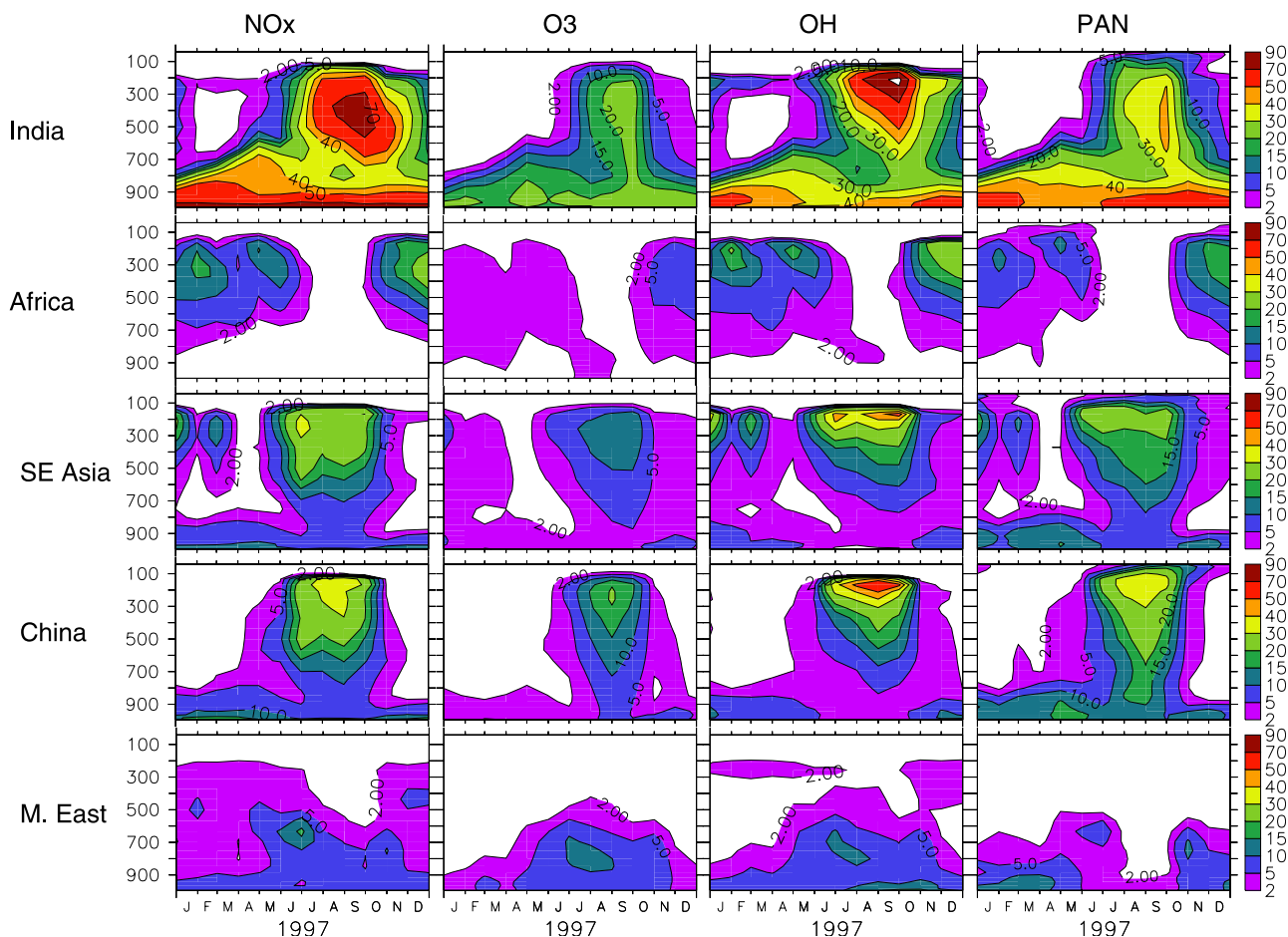|	India	Indonesia	Africa	China	Middle East
January	1.38	1.41	5.10	2.84	0.99
April	2.10	2.02	3.88	3.64	1.10
July	1.66	1.86	5.81	4.68	1.59
October	1.14	1.70	5.88	2.66	1.04
Annual	1.55	1.76	5.30	3.46	1.19

Figure 8. Sensitivity of Indian NO$_x$, O$_3$, OH, and PAN (percent) to NO$_x$ emissions from India, Africa, Southeast Asia, China, and the Middle East.

atmospheric oxidizing efficiency over India through OH. China and the Southeast Asia contribute a sensitivity of ~50% to OH in the UT over India during summer through their NO$_x$ emissions. However, in the LT, throughout the year especially during the winter season, the major contribution is from India.

[35] We also examine the response of the total tropospheric mass of NO$_x$ over India to continental NO$_x$ emissions, which is consistent with the results discussed above, with ~8−10% response to emission from each of Indonesia, China and the Middle East in the LT (Figure 9a). External influence from these regions is largest during the winter season because of the northeasterly trade winds with large-scale subsidence over India. The major influence in the UT is from China and Indonesia (Figure 9b) with a scaled sensitivity of 25−30% each, during the summer monsoon and relatively less (5−10% on average) to emissions from Africa and the Middle East (Figure 9c).

[36] The response of peroxy acetyl nitrate (PAN) to tropospheric NO$_x$ from India and other neighboring continents is also examined. PAN acts as a reservoir species of odd nitrogen during transport to remote regions. It is one of the by-products of photochemical oxidation of NMHCs in the presence of NO$_x$. The lifetime of PAN is about one week in the UT and it depends on NO/NO$_2$ and the temperature. The test results in Figure 8 indicate that ~40−50% of PAN in the surface layer and ~30−40% in the MT during

summer over India is sensitive to local emissions. PAN over India is 10−20% responsive to NO$_x$ emissions from the Middle East and Africa during winter due to SWJ. Twenty to twenty-five percent of PAN over India in the UT is influenced by the NO$_x$ emissions from Southeast Asia and China during the summer monsoon. About 50% of tropospheric PAN over India is sensitive to local NO$_x$ emissions, and this would imply an influence of approximately 50% (mainly in the MT and UT) due to external NO$_x$ emissions. It is found that PAN over India in the MT to UT is insensitive to local NO$_x$ emission from India during winter, indicating the possible influence of external NO$_x$ to India as PAN. During summer, an enhanced sensitivity of PAN over India to emissions from China and Southeast Asia can be seen in the UT.

4.3. Regional Variation of O$_3$ With Respect to NO$_x$ and Nonmethane Hydrocarbon Emissions

[37] The details of NO$_x$ and NMHC emissions employed in the model were explained in section 2, and their individual emission contributions from different sectors over India based on the EDGAR inventory were shown in Figure 3. O$_3$ production depends on NO$_x$ and NMHC emissions in a complex and nonlinear manner depending on their source locations [*Sillman and Samson*, 1999; *Duncan and Chameides*, 1998]. The sensitivity runs for NO$_x$ and NMHCs over India as a whole indicate that regional ozone is strongly
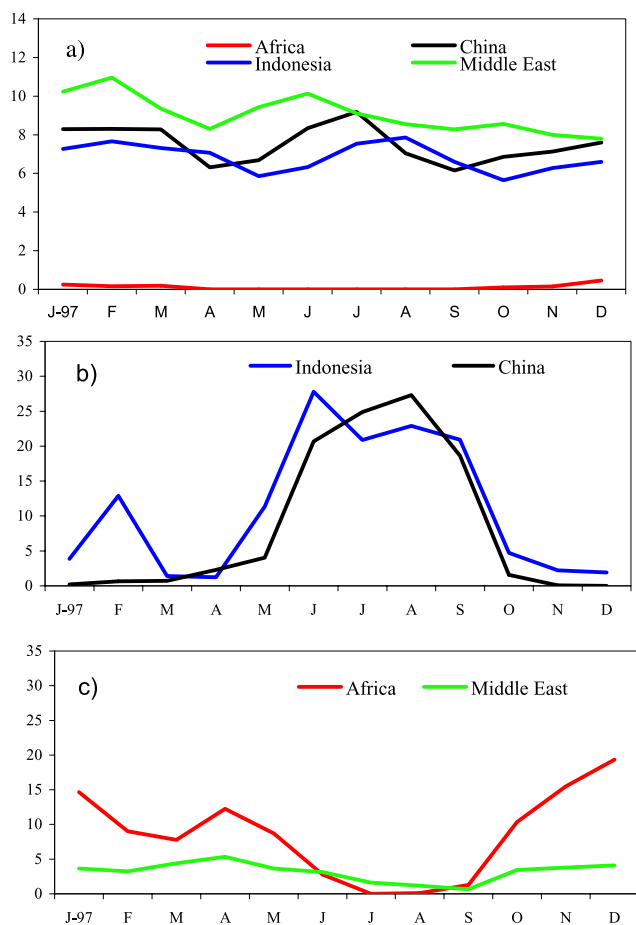
Figure 9. Sensitivity of mass abundance of NO$_x$ (percent) in the (a) lower troposphere (surface to 500 hPa) and (b and c) upper troposphere (500–150 hPa) over India to NO$_x$ emissions from Indonesia, China, Africa, and the Middle East (after four-month model spin-up).

sensitive neither to NO$_x$ nor to NMHCs. However, there are large variations in NO$_x$ and NMHC emissions in different parts of the country from rural to urban regions. This suggests that the generalization of NO$_x$ or NMHC limited regimes as a whole is not very valid over a country like India where the emissions are highly heterogeneous. This may also be influenced by the import of O$_3$ from outside the region. A recent study by *Luo et al.* [2000] suggested that O$_3$ over China is sensitive to both NO$_x$ and VOC over the region but it varies differently from urban to rural areas. An attempt has been made here to understand the regional variation of the response of O$_3$ to emissions by dividing India into different regimes such as North, Central and south India.

[38] The sensitivity of O$_3$ (percent) over these regimes with respect to NO$_x$ emissions (in contours) and NMHC emissions (shaded) are shown in Figure 10. This figure shows that the sensitivity of O$_3$ over southern India with respect to both NO$_x$ and NMHC emissions is relatively stronger than that over northern India. The runs also indicate that the response of O$_3$ to NO$_x$ is larger than to NMHC over all the sub regions. The response is generally more during the summer monsoon, when convection is

stronger and most of the LT NO$_x$ is carried into the UT where the NO$_x$ lifetime is longer, resulting in more O$_3$ formation in the troposphere. The difference in the sensitivity of O$_3$ over south to north is factor of 2 or more with respect to its two precursor emissions (Figure 10). This is partly due to stronger photochemistry with high insolation and humidity over the south as the region is close to the equatorial belt. It is also due to greater present emissions in northern India, so that the chemical system is more saturated with NO$_x$ and responds less to changes in emissions.

5. Discussion and Conclusions

[39] The Indian region is characterized by increasing NO$_x$ emissions with a high energy demand from the increasing population, in addition to natural emissions, which are highly uncertain. As the emissions are heterogeneous with
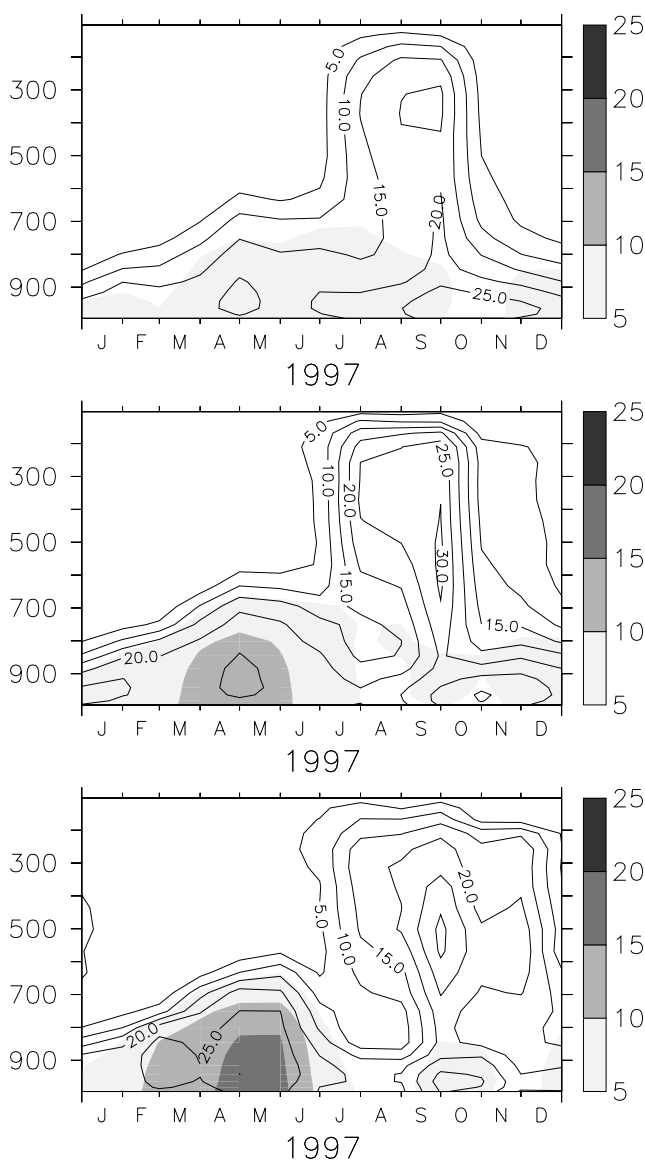

Figure 10. Sensitivity of O$_3$ (percent) over (top) north India, (middle) central India, and (bottom) south India to local NO$_x$ emissions (contours) and NMHC emissions (shaded).

respect to rural and urban India with distinct climatological zones, the limited in situ measurements and field campaigns cannot give an overall picture of the regional NO$_x$ chemistry. In this study, an attempt has been made to understand the NO$_x$ emission and its impact on O$_3$ over India, in light of meteorological features, based on GOME satellite observations and model results from MATCH-MPIC. Model estimates show that the tropospheric mass of NO$_2$ is ∼35% of the stratospheric column over India and varies with respect to seasons, which introduces a difficulty for the satellite estimates of tropospheric columns over this region. The regional NO$_x$ emission strength estimated for India from GOME is 2.35 Tg(N)/yr and is close to the value (2.28 Tg(N)/yr) used in MATCH-MPIC for 1997–1998 with the maximum emissions during April and minimum during the winter months. These values are close to those reported on the basis of sector analysis for India.

[40] The largest response of NO$_x$ to local emissions is 60–70% (in terms of scaled sensitivity) in the LT throughout all seasons and the least response is in the UT during winter. Sensitivity simulations suggest that ∼15–25% of NO$_x$ in the MT and UT over India is sensitive to emissions each from Africa, Southeast Asia and China. Fifty to seventy percent of NO$_x$ in the MT is influenced by local sources during summer. In the LT, the influence from the Middle East is about 10 to 15%. These figures are comparable to the budget of tropospheric mass of NO$_x$ computed for India.

[41] In order to put the simulated O$_3$ sensitivity to NO$_x$ emission into a better perspective, the model simulated O$_3$ was compared with MOZAIC data for 3 Indian airport locations: Delhi, Chennai and Mumbai. Although a direct comparison is difficult between the monthly average model output and the mean of available MOZAIC profiles because of different time sampling and the low resolution of the model data, we found that the model generally overestimates the O$_3$ concentration, while it simulates the seasonal trends well.

[42] O$_3$ over the southern part of India is considerably more sensitive (∼25–30%) than northern India with respect to NO$_x$ and NMHC emissions, largely because of stronger present emissions over northern India. Twenty to twenty-five percent of the BL O$_3$ is sensitive to local NO$_x$ irrespective of the seasonality. The external NO$_x$ influences on Indian O$_3$ are predominantly seen in the MT with a sensitivity of ∼10% each from Southeast Asia and Africa. The oxidizing capacity through OH in the MT and UT over India is significantly influenced by external NO$_x$ emissions from China and Southeast Asia, while the impact of local sources is mainly limited to the LT except in summer. The influence of local NO$_x$ on PAN during winter and the premonsoon is less than 50% and comparatively more (50–80%) during the summer monsoon and the postmonsoon periods.

[43] In conclusion, this study has probed the way to use satellite observations and model output to understand the regional NO$_x$ emission strength and influences on O$_3$-related chemistry over India. However, low fractions of tropospheric mass of NO$_x$ and the influence of external emissions limits the accuracy of this estimate from satellites in addition to the uncertainty with retrievals. O$_3$-related chemistry is very sensitive to southern Asian emissions, but shows large spatial and temporal variation because of

varying lifetime and photochemistry with respect to the seasonal meteorology associated with large-scale transport and mixing.

Appendix A: Small-Perturbation Tendency

[44] The relation between the NO$_x$ concentration and perturbation in NO$_x$ source strength is examined by using the MATCH sensitivity simulations for the Indian region.

[45] Let $X = $ [NO$_x$] be the concentration (molec/m^3) of NO$_x$ and dX/dt be the rate of change of the concentration with respect to time.

[46] For a steady state, $dX/dt = \partial X/\partial t + V\nabla X = 0$, i.e., $X = S/L$, assuming the concentration of NO$_x$ is constant, where S is the source and L is the loss frequency (assumed constant, for the first part of this discussion; changes in L are discussed below).

[47] The source strength

$$S = S_l + S_r,$$

where S_r is the remote source due to flux transport from outside the region and S_l is the direct emission contribution, which is the difference between the local emission and flux out from the region.

$$X = S_l/L + S_r/L. \tag{A1}$$

[48] Let f be the factor that corresponds to different perturbations on the NO$_x$ base source strength S_l and S_l^1 be the new source strength of NO$_x$ in the test run after applying the perturbation. Then

$$S_l^1 = f*S_l \tag{A2}$$

where $f = $ 0, 0.5, 0.8, 0.65, 0.9, 0.99, 1.01, 1.1, 1.35, 1.2, 1.5, and 2 for the runs here.

[49] The ratio of NO$_x$ concentration in the test run to base run can be explained in terms of the local and remote source strength and can be written from equations (A1) and (A2) as

$$X^1/X = \left(S_l^1 + S_r^1\right)/(S_l + S_r) = \left(f*S_l + S_r^1\right)/(S_l + S_r) \tag{A3}$$

where X^1 is the test run NO$_x$ and S_r^1 is the perturbation in the remote source strength of the test run. X is the base run NO$_x$. For this introductory discussion, we assume that the remote source is not changing in the test compared to the base run ($S_r^1 = S_r$), although it is important to note that S_r is not really constant and introduces an important uncertainty in the results, in addition to the uncertainty in the local source strength of the Indian region as compared to remote region source strength.

[50] To derive the relation between the NO$_x$ concentration and perturbation in the NO$_x$ base source strength, let f_1 and f_2 be the factors of two different NO$_x$ perturbations corresponding to the ratios of the test run to base run X_1/X and X_2/X respectively.

[51] Let $k_i = X_i/X$ (from equation (A3)).

$$k_i = (f_i*S_l + S_r)/(S_l + S_r), \text{ where } i = 1, 2 \tag{A4}$$

[52] From equations (A3) and (A4),

$$(k_1 - 1)/(k_2 - 1) = [(f_1 S_l + S_r) - (S_l + S_r)]$$
$$/[(f_2 S_l + S_r) - (S_l + S_r)]$$

$$(k_1 - 1)/(k_2 - 1) = (f_1 - 1)/(f_2 - 1) \qquad \text{(A5)}$$

[53] Equation (A5) indicates that this ratio is independent of the relation between the local (S_l) and remote (S_r) base source strength and depends only on the factor (f) by which the source strength varies with respect to the base source strength, as long as S_r does not change much. Since S_r is only changed because of the changes in gradient, this is expected to hold for small perturbations provided only the local direct emissions are perturbed.

[54] The discussion so far applies only to linear tracers, for which L is constant. For NO$_x$, however, L depends on OH and O$_3$, which in turn depend on NO$_x$, so that it will not be constant. Thus, in contrast to *Wild et al.* [2001], we do not even expect a small perturbation (e.g., 10%) to produce linear effects. However, we do expect the change in OH and O$_3$, and thus in L, to be approximately linear for small perturbations: If a reduction in NO$_x$ emissions by 1% causes a reduction in OH by 0.5%, then we would expect that a reduction of 2% in the emissions results in an OH reduction of 1%. For large changes, however, the entire photochemical regime can shift (e.g., low NO$_x$ versus high NO$_x$) leading to a departure from this small-perturbation tendency (SPT).

[55] The model simulated NO$_x$ column abundance for the period December 1996 (after a three-month spin-up) is analyzed by increasing/decreasing the source strength by 1%, 10%, 20%, 35%, 50% and 100% and the ratio of the new abundance with respect to base run is computed for the period. The difference of the ratio with unity ($x_1/x - 1$) and the perturbation factor with unity ($f - 1$) is analyzed for different vertical columns to see the departure from the SPT (Table 4).

References

Akimoto, H. (2003), Global air quality and pollution, *Science*, 302, 1716–1719.

Beirle, S., U. Platt, M. Wenig, and T. Wagner (2004), NO$_x$ production by lightning estimated with GOME, *Adv. Space Res.*, 34, 793–797.

Burrows, J. P., M. Weber, M. Buchwitz, V. V. Rozanov, A. Ladstätter-Weißenmayer, A. Richter, R. DeBeek, R. Hoogen, K. Brmstedt, and K. U. Eichmann (1999), The Global Ozone Monitoring Experiment (GOME): Mission concept and first scientific results, *J. Atmos. Sci.*, 56, 151–175.

Burrows, J. P., A. Richter, and L. Hild (2004), Studies of NO$_2$ from lightning and convective uplifting using GOME data, in *Sounding the Troposphere From Space: A New Era for Atmospheric Chemistry*, edited by P. Borrell, J. P. Burrows, and U. Platt, pp. 297–306, Springer, New York.

Carmichael, G. R., I. Uno, M. J. Phadnis, Y. Zhang, and Y. Sunwoo (1998), Tropospheric ozone production and transport in the springtime east Asia, *J. Geophys. Res.*, 103, 10,649–10,671.

Chameides, W. L., and J. C. G. Walker (1973), A photochemical theory of tropospheric ozone, *J. Geophys. Res.*, 78, 8751–8760.

Chand, D., and S. Lal (2004), High ozone at rural sites in India, *Atmos. Chem. Phys. Discuss.*, 4, 3359–3380.

Crutzen, P. J. (1974), Photochemical reactions initiated by and influencing ozone in unpolluted tropospheric air, *Tellus*, 26, 48–57.

Crutzen, P. J., and M. G. Lawrence (2000), The impact of precipitation scavenging on the transport of trace gases: A 3-dimensional model sensitivity study, *J. Atmos. Chem.*, 37, 81–112.

Dentener, F. J., and P. J. Crutzen (1993), Reaction of N$_2$O$_5$ on tropospheric aerosols: Impact on the global distributions of NO$_x$, O$_3$, and OH, *J. Geophys. Res.*, 98, 7149–7163.

Duncan, B. N., and W. L. Chameides (1998), Effects of urban emission control strategies on the export of ozone and ozone precursors from the urban atmosphere to the troposphere, *J. Geophys. Res.*, 103, 28,159–28,180.

Duncan, B. N., R. V. Martin, A. C. Staudt, R. Yevich, and J. A. Logan (2003), Interannual and seasonal variability of biomass burning emissions constrained by satellite observations, *J. Geophys. Res.*, 108(D2), 4100, doi:10.1029/2002JD002378.

Fishman, J., S. Solomon, and P. J. Crutzen (1979), Observational and theoretical evidence in support of a significant in-situ photochemical source of tropospheric ozone, *Tellus*, 31, 432–446.

Gadi, R., U. C. Kulshrestha, A. K. Sarkar, S. C. Garg, and D. C. Parashar (2003), Emissions of SO$_2$ and NO$_x$ from biofuels in India, *Tellus, Ser. B*, 55(3), 787–795.

Garg, A., P. R. Shukla, S. Bhattacharya, and V. K. Dadhwal (2001), Sub-region (district) and sector level SO$_2$ and NO$_x$ emissions for India: Assessment of inventories and mitigation flexibility, *Atmos. Environ.*, 35, 703–713.

Horowitz, L. W., and D. J. Jacob (1999), Global impact of fossil fuel combustion on atmospheric NO$_x$, *J. Geophys. Res.*, 104, 23,823–23,840.

Jaffe, D., et al. (1999), Transport of Asian air pollution to North America, *Geophys. Res. Lett.*, 26, 711–714.

Kalnay, E., et al. (1996), The NCEP/NCAR 40-Year Reanalysis Project, *Bull. Am. Meteorol. Soc.*, 77, 437–471.

Kunhikrishnan, T. (2004), *Synergetic Use of a Global 3D Chemistry and Meteorology Model and Satellite Observations for the Study of Tropospheric NO$_x$-Related Chemistry Over Asia and the Indian Ocean*, Ber. Inst. Umweltphys., vol. 23, 242 pp., Logos Verlag, Berlin.

Kunhikrishnan, T., and M. G. Lawrence (2004), Sensitivity of NO$_x$ over the Indian Ocean to emissions from the surrounding continents and nonlinearities in atmospheric chemistry responses, *Geophys. Res. Lett.*, 31, L15109, doi:10.1029/2004GL020210.

Kunhikrishnan, T., M. G. Lawrence, R. von Kuhlmann, A. Richter, A. Ladstaetter-Weissenmayer, and J. P. Burrows (2004a), Analysis of tropospheric NO$_x$ over Asia using the model of atmospheric transport and chemistry (MATCH-MPIC) and GOME-satellite observations, *Atmos. Environ.*, 38, 581–596.

Kunhikrishnan, T., M. G. Lawrence, R. von Kuhlmann, A. Richter, A. Ladstätter-Weißenmayer, and J. P. Burrows (2004b), Semiannual NO$_2$ plumes during the monsoon transition periods over the central Indian Ocean, *Geophys. Res. Lett.*, 31, L08110, doi:10.1029/2003GL019269.

Lacis, A. A., D. J. Wuebbles, and J. A. Logan (1990), Radiative forcing of climate by changes in the vertical distribution of ozone, *J. Geophys. Res.*, 95, 9971–9981.

Lal, S., M. Naja, and B. H. Subbaraya (2000), Seasonal variations in surface ozone and its precursors over an urban site in India, *Atmos. Environ.*, 34, 2713–2724.

Law, K. S., P. H. Plantevin, D. E. Shallcross, H. L. Rogers, J. A. Pyle, C. Grouhel, V. Thouret, and M. Marenco (1998), Evaluation of modeled O$_3$ using measurement of Ozone by Airbus In-Service Aircraft (MOZAIC) data, *J. Geophys. Res.*, 103, 25,721–25,737.

Lawrence, M. G. (2004), Export of air pollution from southern Asia and its large-scale effects, in *Handbook of Environmental Chemistry*, vol. 4, edited by A. Stohl, pp. 131–172, Springer, New York.

Lawrence, M. G., P. J. Crutzen, P. J. Rasch, B. E. Eaton, and N. M. Mahowald (1999), A model for studies of tropospheric photochemistry: Description, global distributions and evaluation, *J. Geophys Res.*, 104, 26,245–26,277.

Lawrence, M. G., et al. (2003), Global chemical weather forecasts for field campaign planning: Predictions and observations of large-scale features during INDOEX, MINOS, and CONTRACE, *Atmos. Chem. Phys.*, 3, 267–289.

Leue, C., M. Wenig, T. Wagner, O. Klimm, U. Platt, and B. Jähne (2001), Quantitative analysis of NO$_x$ emissions from Global Ozone Monitoring Experiment satellite image sequences, *J. Geophys. Res.*, 106, 5493–5506.

Levy, H., W. J. Moxim, A. A. Klonecki, and P. S. Kasibhatla (1999), Simulated tropospheric NO$_x$: Its evaluation, global distribution and individual source contributions, *J. Geophys. Res.*, 104, 26,279–26,306.

Luo, C., J. John, Z. Xiuji, K. Lam, T. Wang, and W. Chameides (2000), A nonurban ozone air pollution episode over eastern China: Observations and model simulations, *J. Geophys. Res.*, *105*, 1889–1908.

Marenco, A., et al. (1998), Measurement of Ozone and Water Vapor by Airbus In-service Aircraft: The MOZAIC airborne program, an overview, *J. Geophys. Res.*, *103*, 25,631–25,642.

Martin, R. V., et al. (2002), An improved retrieval of tropospheric nitrogen dioxide from GOME, *J. Geophys. Res.*, *107*(D20), 4437, doi:10.1029/2001JD001027.

Martin, R. V., D. J. Jacob, K. Chance, T. P. Kurosu, P. I. Palmar, and M. J. Evans (2003), Global inventory of nitrogen oxide emissions constrained by space-observed observations of NO$_2$ columns, *J. Geophys. Res.*, *108*(D17), 4537, doi:10.1029/2003JD003453.

Mitra, A. P., and C. Sharma (2002), Indian aerosols: Present status, *Chemosphere*, *49*, 1175–1190.

Olivier, J. G. J., J. P. J. Bloos, J. J. M. Berdowski, A. J. H. Visschedijk, and A. F. Bouwman (1999), A 1990 global emission inventory of anthropogenic sources of carbon monoxide on 1° × 1° developed in the framework of EDGAR/GEIA, *Chemosphere Global Change Sci.*, *1*, 1–17.

Rasch, P. J., N. M. Mahowald, and B. E. Eaton (1997), Representations of transport, convection and the hydrologic cycle in chemical transport models: Implications for the modeling of short lived and soluble species, *J. Geophys. Res.*, *102*, 28,127–28,138.

Richter, A., and J. P. Burrows (2002), Retrieval of tropospheric NO$_2$ from GOME measurements, *Adv. Space Res.*, *29*, 1673–1683.

Richter, A., V. Eyring, J. P. Burrows, H. Bovensmann, A. Lauer, B. Sierk, and P. J. Crutzen (2004), Satellite measurements of NO$_2$ from international shipping emissions, *Geophys. Res. Lett.*, *31*, L23110, doi:10.1029/2004GL020822.

Sharma, C., A. Dasgupta, and A. P. Mitra (2002), Future scenarios of inventories of GHGs and urban pollutants from Delhi and Calcutta, paper presented at IGES/APN Mega-City Project Workshop, Inst. for Global Environ. Strategies, Kitakyushu, Japan, 23–25 Jan.

Sillman, S., and P. J. Samson (1999), Impact of temperature on oxidant photochemistry in urban, polluted rural and remote environments, *J. Geophys. Res.*, *100*, 11,497–11,508.

Streets, D. G., and S. T. Waldhoff (1999), Biofuel use in Asia and acidifying emissions, *Energy*, *23*, 1029–1042.

Streets, D. G., K. F. Yarber, J.-H. Woo, and G. R. Carmichael (2003), Biomass burning in Asia: Annual and seasonal estimates and atmospheric emissions, *Global Biogeochem. Cycles*, *17*(4), 1099, doi:10.1029/2003GB002040.

Thouret, V., A. Marenco, J. Logan, P. Nedelec, and C. Grouhel (1998), Comparisons of ozone measurements from MOZAIC airborne program and the ozone sounding network at eight locations, *J. Geophys. Res.*, *103*, 25,695–25,720.

United Nations Environment Programme (UNEP) (2002), Air pollution and ozone, in *The Asian Brown Cloud: Climate and Other Environmental Impacts, Assess. Rep. UNEP/DEWA/RS.02-3*, chap. 3, pp. 16–20, Nairobi.

van Aardenne, J. A., G. R. Carmichael, H. Levy II, D. Streets, and L. Hordijk (1999), Anthropogenic NO$_x$ emission in Asia in the period 1990–2020, *Atmos. Environ.*, *33*, 633–646.

Varshney, C. K., and M. Agarwal (1992), Ozone levels in the urban atmosphere of Delhi, *Atmos. Environ., Part B*, *26*, 291–294.

von Kuhlmann, R., M. G. Lawrence, P. J. Crutzen, and P. J. Rasch (2003a), A model for studies of tropospheric ozone and nonmethane hydrocarbons: Model description and ozone results, *J. Geophys. Res.*, *108*(D9), 4294, doi:10.1029/2002JD002893.

von Kuhlmann, R., M. G. Lawrence, Crutzen, and P. J. Rasch (2003b), A model for studies of tropospheric ozone and nonmethane hydrocarbons: Model evaluation of ozone related species, *J. Geophys. Res.*, *108*(D23), 4729, doi:10.1029/2002JD003348.

Wenig, M. (2001), Satellite measurements of long-term global tropospheric trace gas distributions and source strengths: Algorithm development and data analysis, Ph.D. thesis, Rupertus Carola Univ. of Heidelberg, Heidelberg, Germany.

Wild, O., M. J. Prather, and H. Akimoto (2001), Indirect long-term global radiative cooling from NO$_x$ emissions, *Geophys. Res. Lett.*, *28*, 1719–1722.

Yienger, J. J., M. Galanter, T. A. Holloway, M. J. Phadnis, S. K. Guttikunda, G. R. Carmichael, W. J. Moxim, and H. Levy II (2000), The episodic nature of air pollution transport from Asia to North America, *J. Geophys. Res.*, *105*, 26,931–26,946.

———————————

W. A. H. Asman and M. G. Lawrence, Department of Atmospheric Chemistry, Max Planck Institute for Chemistry, Postfach 3060, D-55020 Mainz, Germany.

J. P. Burrows and A. Richter, Department of Environmental Physics and Remote Sensing, University of Bremen, D-28359 Bremen, Germany.

T. Kunhikrishnan, Atmospheric Science Directorate, NASA Langley Research Center, 100 NASA Road, Hampton, VA 23681, USA. (kunhi@larc.nasa.gov)

R. von Kuhlmann, German Aerospace Center, Königswinterer Strasse 522-524, D-53227 Bonn, Germany.

M. O. Wenig, NASA Goddard Space Flight Center, Greenbelt, MD 20771, USA.